Developmental Biology 434 (2018) 221–230

Contents lists available at ScienceDirect

Developmental Biology

journal homepage: www.elsevier.com/locate/developmentalbiology

Original research article

ZYG-1 promotes limited centriole amplification in the *C. elegans* seam lineage

Benita Wolf, Fernando R. Balestra[1], Antoine Spahr, Pierre Gönczy[*]

Swiss Institute for Experimental Cancer Research (ISREC), School of Life Sciences, Swiss Federal Institute of Technology (EPFL), Lausanne, Switzerland

ARTICLE INFO

Keywords:
C. elegans
Seam cells
Centrosome
Centriole
Amplification
Aneuploidy

ABSTRACT

Genome stability relies notably on the integrity of centrosomes and on the mitotic spindle they organize. Structural and numerical centrosome aberrations are frequently observed in human cancer, and there is increasing evidence that centrosome amplification can promote tumorigenesis. Here, we use *C. elegans* seam cells as a model system to analyze centrosome homeostasis in the context of a stereotyped stem like lineage. We found that overexpression of the Plk4-related kinase ZYG-1 leads to the formation of one supernumerary centriolar focus per parental centriole during the cell cycle that leads to the sole symmetric division in the seam lineage. In the following cell cycle, such supernumerary foci function as microtubule organizing centers, but do not cluster during mitosis, resulting in the formation of a multipolar spindle and then aneuploid daughter cells. Intriguingly, we found also that supernumerary centriolar foci do not assemble in the asymmetric cell divisions that precedes or that follows the symmetric seam cell division, despite the similar presence of GFP::ZYG-1. Furthermore, we established that supernumerary centrioles form earlier during development in animals depleted of the heterochronic gene *lin-14*, in which the symmetric division is precocious. Conversely, supernumerary centrioles are essentially not observed in animals depleted of *lin-28*, in which the symmetric division is lacking. These findings lead us to conclude that ZYG-1 promotes limited centriole amplification solely during the symmetric division in the *C. elegans* seam lineage.

1. Introduction

The centrosome is the major microtubule-organizing center (MTOC) of animal cells, and as such plays fundamental roles in organizing the microtubule cytoskeletal network, including the mitotic spindle (reviewed in Bornens, 2012; Woodruff et al., 2014). Although the available evidence indicates that centrosome number needs to be tightly regulated to achieve proper cell architecture and genome stability, the consequences of centrosome numerical aberrations for stem cell lineages in developing organisms remain incompletely understood.

In most animal cells, centrosomes assemble around centrioles, which are minute microtubule-based cylindrical organelles (reviewed in Brito et al., 2012; Firat-Karalar and Stearns, 2014; Gönczy, 2012). Early in the cell cycle, there are two centrioles that are usually located close to one another and which recruit the pericentriolar material (PCM) that nucleates most cellular microtubules. Typically at the transition between the G1 and the S phases of the cell cycle, a procentriole assembles next to each parental centriole and remains tightly engaged with it. During mitosis, the PCM surrounding the two pairs of centriole/procentriole directs assembly of the bipolar spindle, thereby contributing to faithful chromosome segregation. During anaphase, the centriole and procentriole within each pair disengage from one another, thus endowing each daughter cell with two centriolar cylinders and completing the centriole duplication cycle.

Work in *C. elegans* embryos has uncovered six evolutionarily conserved components that are essential for procentriole assembly: SAS-7 (Sugioka et al., 2017), SPD-2 (Dammermann et al., 2004; Kemp et al., 2004), ZYG-1 (O'Connell et al., 2001), SAS-6 (Dammermann et al., 2004; Leidel et al., 2005), SAS-5 (Dammermann et al., 2004; Delattre et al., 2004) and SAS-4 (Kirkham et al., 2003; Leidel and Gönczy, 2003). In other systems, including human cells, overexpression of homologues of ZYG-1, SAS-6 or SAS-5 results in the assembly of up to 6 supernumerary procentrioles around each parental centriole (Arquint et al., 2012; Comartin et al., 2013; Habedanck et al., 2005; Strnad et al., 2007). Such experimentally induced amplification of centriole number has allowed addressing the consequences of harboring too many centrosomes in cells and organisms. For example,

* Corresponding author.
E-mail address: pierre.gonczy@epfl.ch (P. Gönczy).
[1] Present address: Cell Dynamics and Signaling Department, CABIMER-CSIC/US/UPO, 41092-Seville, Spain.

https://doi.org/10.1016/j.ydbio.2018.01.001
Received 8 September 2017; Received in revised form 8 December 2017; Accepted 1 January 2018
Available online 04 January 2018

overexpression of the ZYG-1-related protein Polo-like-kinase 4 (Plk4) in human tissue culture cells results in the presence of extra centrosomes, which usually cluster into two ensembles during mitosis, thus enabling bipolar spindle assembly (Ganem et al., 2009; Kwon et al., 2008; Quintyne et al., 2005; Silkworth et al., 2009).

This clustering mechanism does not ensure faithful chromosome segregation, however, as the frequency of merotelic attachments is dramatically augmented in such cells, leading to genome instability (Ganem et al., 2009; Silkworth et al., 2009). Overexpression of Plk4 in *Drosophila* (DmPlk4) also results in extra centrosomes that cluster in a robust manner during mitosis, so that centrosome number aberrations are of little consequence to the organism (Basto et al., 2008). Nevertheless, the asymmetric division of neural stem cells is compromised in such flies, and tumor formation can be initiated by transplanting cells overexpressing DmPlk4 into the abdomen of a host fly (Basto et al., 2008). Importantly, in addition, induction of excess centrosomes via Plk4 overexpression is sufficient to promote aneuploidy and tumor initiation in multiple tissues of the mouse (Levine et al., 2017) as well as tissue hyperplasia in the mouse epidermis (Coelho et al., 2015), leading to tumor formation in the absence of p53 (Sercin et al., 2016). This is not the case in all organs, however. For instance, in the developing mouse neocortex, Plk4-mediated centrosome amplification results in multipolar spindle assembly, presumably owing to less efficient clustering mechanisms (Marthiens et al., 2013). In turn, this leads to aneuploid daughter cells and, ultimately, to the depletion of neuronal cells and microcephaly (Marthiens et al., 2013).

Somewhat paradoxically considering that the core components driving procentriole assembly have been discovered in *C. elegans*, the consequence of excess centrosomes has not been investigated in somatic cells of the worm thus far, including in the seam stem cell like lineage. Seam cells are neuroectodermal cells present in lateral rows on the side of worm larvae (reviewed in Joshi et al., 2010). Embryos hatch with 10 seam cells on each side of the animal, called H0, H1, H2, V1, V2, V3, V4, V5, V6 and T (Fig. 1A, B). These cells and their descendants follow a stereotypical stem like lineage during the four larval stages that comprises several asymmetric divisions, which yield another posteriorly located seam cell (referred to as a stem cell hereafter for simplicity) and an anteriorly located differentiating cell that fuses with the hypodermal syncytium (Fig. 1B). In addition, a single symmetric division occurs at the onset of the second larval stage in V1, V2, V3, V4, V6 and H1, which increases the stem cell pool from 10 to 16 on each side of the animal (Fig. 1B dark blue). At the end of the fourth larval stage, all cells differentiate and fuse with the hypodermal syncytium.

Three modules are known to regulate seam cell fate, and, thereby, the number of cells eventually produced by the entire lineage. First, Wnt signaling determines the polarity of the asymmetric divisions along the anterior-posterior (A-P) axis, ultimately by controlling the ratio between the Wnt effector POP-1 and its coactivator SYS-1 in the two daughter cells (reviewed in Mizumoto and Sawa, 2007). Accordingly, disruption of Wnt pathway components leads to fate alterations and abnormal seam cell numbers (Gleason and Eisenmann, 2010). Second, several transcription factors, including RNT-1 and BRO-1, as well as CEH-20 and UNC-62, regulate seam cell fate independently of Wnt signaling (reviewed in Nimmo and Woollard, 2008). For example, RNT-1/BRO-1 promote the proliferative fate of posterior daughters by inhibiting the cyclin E/CDK-2 inhibitor CKI-1 (Kagoshima et al., 2007, 2005; Nimmo et al., 2005). A third module that contributes to proper seam cell number is that of the heterochronic gene network, which controls the timing of select developmental events in *C. elegans* larvae (reviewed in Ambros, 2000; Pasquinelli and Ruvkun, 2002). When the function of genes in this network is missing, whole larval stages are skipped or, instead, reiterated. For instance, the presence of LIN-14 in L1 larvae prevents the adoption of L2 fates, which are acquired only after *lin-14* function has been downregulated by the *lin-4* microRNA (Ha et al., 1996). Thus, in *lin-14* loss of function mutants, L1-specific events are missing and L2-specific events, including the symmetric division, occur precociously (Ambros and Horvitz, 1984, 1987; Chalfie et al., 1981). Another *lin-4* microRNA target, the RNA-binding protein LIN-28, is a positive regulator of L2 fates, including the symmetric division. Accordingly, L2-specific events are skipped and subsequent events occur earlier relative to the wild type in *lin-28* null mutants (Ambros, 1989; Ambros and Horvitz, 1984; Moss et al., 1997; Vadla et al., 2012).

In this study, we sought to provoke the presence of extra centrosomes in *C. elegans* seam cells to uncover the resulting consequences in the context of this stereotyped stem cell lineage.

2. Results

2.1. Centrosomes direct spindle assembly in C. elegans seam cells

We set out to analyze centrioles in the seam cell lineage and ascertain whether they function to organize centrosomes and, thereby, direct spindle assembly. Throughout this work, we focus our analysis on the V1, V2, V3, V4 and V6 lineages, hereafter referred to collectively as "V(n) lineage" for simplicity, in which division patterns are comparable and regulated in a similar manner (Fig. 1A, B, Fig. S1A (Sulston and Horvitz, 1977, 1981)).

To monitor centrioles in seam cells, we generated a transgenic line expressing GFP::SAS-4 under a seam cell promoter; such expression was of no consequence to centriole numbers (data not shown and see below). These transgenic animals also express mCherry::H2B to label chromatin in seam cells, as well as YFP to mark differentiated hyp7 cells (Fig. 1A, Fig. S1B; hereafter referred to as "control strain -ctrl", see Materials and Methods for all worm strains utilized in this study). Wide field live imaging of control larvae established the presence of GFP::SAS-4 foci throughout the seam lineage (Fig. 1B-H). We found that seam cells typically harbored a single GFP::SAS-4 focus during interphase (Fig. 1C), as anticipated from the fact that the two centrioles, which are merely ~150 nm-long in nematodes (Wolf et al., 1978) are too close to one another to be distinguished as single entities by conventional microscopy. Nevertheless, two GFP::SAS-4 foci could sometimes be detected, probably in interphase cells that had advanced in the cell cycle (Fig. 1F, Fig. S1B inset for V6p). During mitosis, a single focus of GFP::SAS-4 was usually present on either side of the metaphase plate (Fig. 1D, G), each presumably corresponding to a centriole/procentriole pair at the two poles of the mitotic spindle. During anaphase, the centriole/procentriole within each pair disengaged from one another, so that typically four GFP::SAS-4 foci could be observed per cell, two at each spindle pole (Fig. 1E, H). The above sequence of events was observed both during the symmetric division in early L2 larvae (V(n)p, Fig. 1C-E), as well as during the asymmetric divisions that precede (V(n)) and follow (V(n)pp/pa), respectively (data not shown and Fig. 1F-H).

To address whether GFP::SAS-4 foci observed in seam cells correspond to *bona fide* centrioles, as opposed to aggregates of the fusion protein, we performed immunofluorescence analysis to examine the distribution of the endogenous centriolar proteins SAS-6, SAS-5 and SAS-4, and found them to co-localize with GFP::SAS-4 (Fig. 1I-K). Overall, we conclude that centrioles are present in seam cells and that they undergo a canonical duplication cycle.

We wanted to test whether centrioles are essential to organize centrosomes and direct spindle assembly in seam cells. We found that, instead of bipolar spindles that segregate chromosomes towards the two daughter cells (Fig. 1L), monopolar configurations with chromosomes arranged in a circular manner were present in larvae stemming from hermaphrodites treated with *sas-6(RNAi)* (Fig. 1M, N). Filming of such cells revealed cell division failure (Fig. S2A), likely explaining the consequent larger size of nuclei following SAS-6 depletion (compare Fig. 1L and M). Findings compatible with such defects were made in worms carrying the null allele *sas-6(ok2554)* or the strong loss-of-

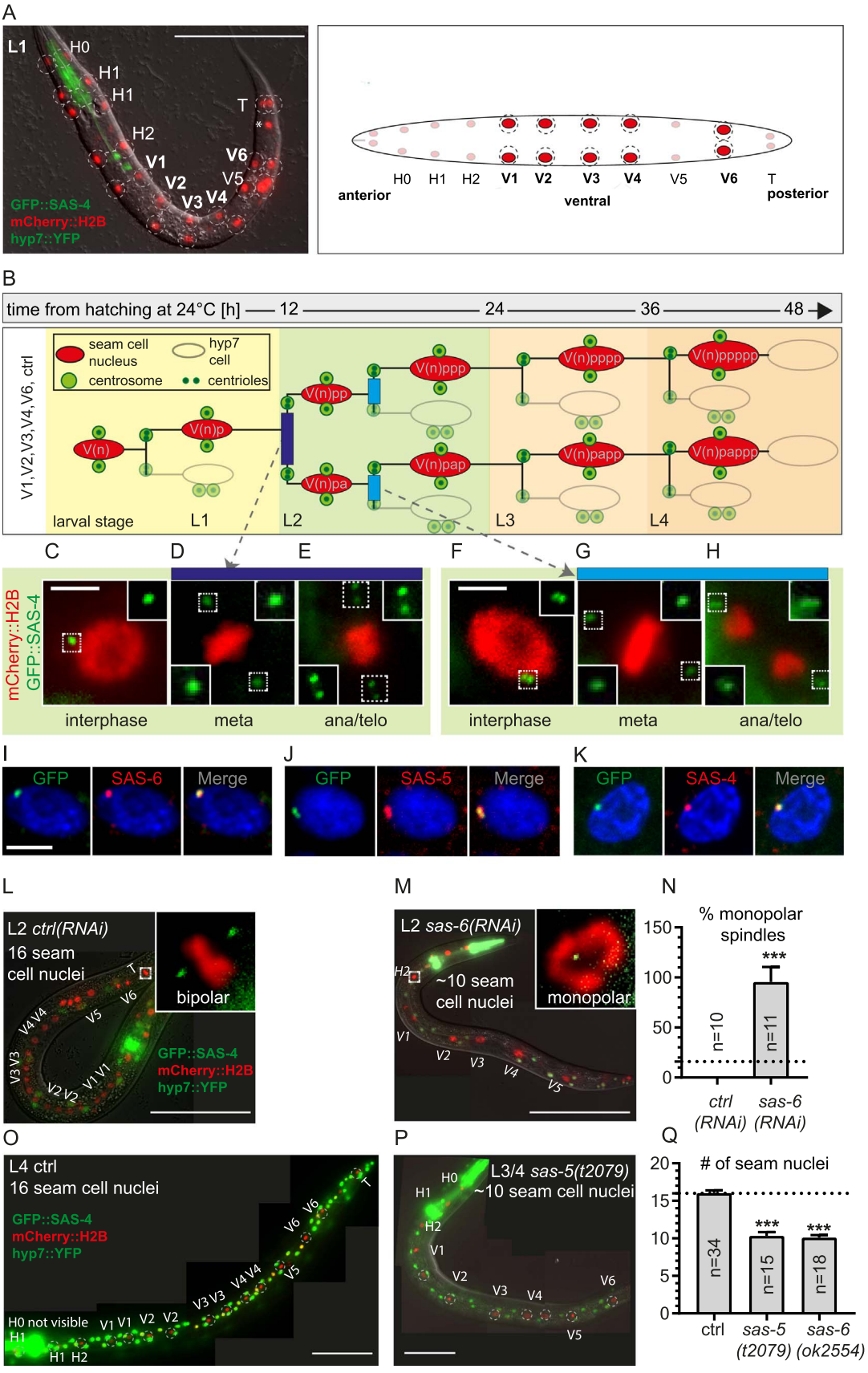
A
L1
H0
H1
H1
H2
V1
V2
V3
V4
V5
V6
T
GFP::SAS-4
mCherry::H2B
hyp7::YFP
anterior
posterior
ventral
B
time from hatching at 24°C [h]
12
24
36
48
seam cell nucleus
hyp7 cell
centrosome
centrioles
V1,V2,V3,V4,V6, ctrl
V(n)
V(n)p
V(n)pp
V(n)pa
V(n)ppp
V(n)pap
V(n)pppp
V(n)papp
V(n)ppppp
V(n)pappp
larval stage
L1
L2
L3
L4
C
D
E
F
G
H
mCherry::H2B
GFP::SAS-4
interphase
meta
ana/telo
I
J
K
GFP
SAS-6
SAS-5
SAS-4
Merge
L
L2 ctrl(RNAi)
16 seam cell nuclei
bipolar
M
L2 sas-6(RNAi)
~10 seam cell nuclei
monopolar
N
% monopolar spindles
n=10
n=11
ctrl (RNAi)
sas-6 (RNAi)
O
L4 ctrl
16 seam cell nuclei
H0 not visible
P
L3/4 sas-5(t2079)
~10 seam cell nuclei
Q
# of seam nuclei
n=34
n=15
n=18
ctrl
sas-5 (t2079)
sas-6 (ok2554)

Fig. 1. Centrioles direct proper division of *C. elegans* seam cells. A Still image from live recording of L1 larva expressing mCherry::H2B (red, chromatin) and GFP::SAS-4 (green, centrioles, not visible at this magnification) in seam cells, as well as hyp7::YFP to mark hypodermal cells (green, seen only in the pharynx in L1 larvae) (left), with corresponding schematic representation (right, only seam cell nuclei are depicted). The names of the seam cell lineages are shown; H: head, V: ventral, T: tail; shown in bold are the V(n) lineages analyzed in this work. Scale bar: 100 μm. * indicates a cell that is not part of the seam cell lineage but which expresses mCherry::H2B due to a leaky promoter (visible only in L1). **B** Schematic representation of seam cell division pattern across larval development for V1, V2, V3, V4 and V6 lineages (V(n)) in control (ctrl) animals. Time after hatching at 24 °C is indicated. Represented are seam cell nuclei (red) and differentiating hyp7 cells (empty circles) in the L1, L2, L3 and L4 larval stages, as well as centrioles and centrosomes, as indicated; a: anterior, p: posterior. Dark blue rectangle indicates the symmetric division of V(n)p cells, lighter blue rectangles the subsequent asymmetric division of V(n)pp/pa cells. **C-H** Still images from different live larvae expressing mCherry::H2B (red, nuclei) and GFP::SAS-4 (green, centrioles) in seam cells; shown are V(n)p cells, which undergo symmetric division **(C-E),** as well as V(n)pa/ V(n)pp cells, which undergo asymmetric division meta: metaphase, ana/telo: anaphase/telophase, in this and other figures. Scale bar: 10 μm. **I-K** Dual immunofluorescence analysis of V4pp interphase cell expressing notably GFP::SAS-4 in seam cells, using antibodies against GFP (green) and against SAS-6 **(I)**, SAS-5 **(J)** or SAS-4 **(K)**, all visible in red; DNA is shown in blue. Scale bar: 10 μm. **L, M** Still images from live recordings of L2 larvae expressing in seam cells mCherry::H2B (red, chromosomes, DNA) and GFP::SAS-4 (visible in insets), as well as hyp7::YFP (green, hypodermis), in a control RNAi condition **(L)** or upon *sas-6(RNAi)* **(M)**. Insets show higher magnification views of a cell undergoing biopolar spindle assembly (**L**) or monopolar spindle assembly (**M**). Scale bar: 100 μm. **N** Quantification of the percentage of monopolar spindles observed in ctrl animals and upon *sas-6(RNAi)* 36 h after the onset of RNAi; Student's *t*-test with Welch correction, *** $p < 0.001$; 9 worms each yielding 10 and 11 mitotic cells, respectively, were scored. **O, P** Still images from live recordings of worms expressing in seam cells mCherry::H2B (red, chromosomes, DNA) and GFP::SAS-4 (not visible at this magnification), as well as hyp7::YFP (green, hypodermis), in a control condition (**O**) or in a *sas-5*(*t2079*) mutant background **(P)**, T lineage not visible in **(P)**. Dashed circles indicate seam cells of relevant lineages (V1, V2, V3, V4, V6). Upon *sas-5* inactivation, we usually found 1 seam cell per lineage (V1, V2, V3, V6) in L3/L4 larvae, suggesting that the symmetric seam cell division had failed **(P).** Scale bar: 100 μm. **Q** Quantification of seam cell number from live recordings of control, *sas-6*(*ok2554*) and *sas-5*(*t2079*) animals; Student's *t*-test with Welch correction, *** $p < 0.001$. Worms were scored 20 h after hatching, when 16 seam cells are already present in ctrl conditions.

function allele *sas-5(t2079)*: although no difference with control worms was noted in L1 larvae, presumably owing to the remaining maternal protein pool, cell division failure was observed thereafter upon live imaging of worms (Fig. S2B for *sas-6(ok2554)*; see Fig. 1P for *sas-5(t2079)*). Probably as a consequence, we found that whereas there were 16 seam cell nuclei on average per side in control animals at the end of larval development, there were approximately 10 in *sas-6(ok2554)* or *sas-5(t2079)* mutant animals (Fig. 1O-Q). Likewise, the average number of hyp7 cells, which was determined solely in the *sas-5(t2079)* mutant background, was decreased (Fig. 1P, Fig. S2C).

Together, the above findings establish that correct centriole number is needed for bipolar spindle assembly in seam cells, as well as for generating correct cell numbers in both seam and hypodermal lineages. Furthermore, these findings indicate that the mechanisms that enable spindle assembly to occur independently of centrosomes in some systems do not operate robustly enough here to compensate for diminished centrosome numbers.

2.2. Expression of GFP::ZYG-1 promotes limited centriole amplification in seam cells

We next sought to induce the formation of supernumerary centrioles in seam cells by providing an excess of the Plk4-related kinase ZYG-1. To this end, we drove expression of *gfp::zyg-1* from a seam cell promoter in worms also expressing mCherry::H2B in seam cells and YFP in hyp7 cells (for simplicity, this strain is referred to as GFP::ZYG-1 hereafter). We synchronized animals as L1 larvae and counted the number of centriolar foci marked by GFP::ZYG-1 (Fig. 2). We found that there were no more than 2 centriolar foci in interphase and no more than 4 centriolar foci in anaphase in both control and GFP::ZYG-1 in the V(n) cells of L1 larvae (Fig. S2D, see Fig. 1B). During interphase of the next, V(n)p, cell cycle, a maximum of 2 centriolar foci were likewise detected in both control and GFP::ZYG-1 animals (Fig. 2A, G “interphase”). However, a striking phenotype became apparent sometimes already in metaphase and usually in anaphase/telophase of V(n)p cells, with ~66% of GFP::ZYG-1 cells exhibiting more than the normal number of 4 centriolar foci (Fig. 2C, G “ana/telo”, J). We noted also that triplets of centriolar foci were present per spindle pole in ~97% of anaphase figures exhibiting amplification (Fig. 2C), indicating that just one supernumerary procentriole assembled per parental centriole. Furthermore, immunofluorescence experiments established that supernumerary foci harboring GFP::ZYG-1 also contained the endogenous centriolar proteins SAS-6, SAS-5 and SAS-4 (Fig. 2K-M). We conclude that providing ZYG-1 in excess results in the formation of one additional procentriole per parental centriole during the V(n)p cell cycle that leads to the sole symmetric division in the seam cell lineage.

What happens to supernumerary centrioles induced by the presence of GFP::ZYG-1 in the following cell cycle, that of V(n)pp/pa? We found that ~77% of GFP::ZYG-1 V(n)pp/pa interphase cells had more than 2 centriolar foci, usually 3, as anticipated following the disengagement of 2 procentrioles from one parental centriole during the preceding V(n)p mitosis (Fig. 2D), with the remainder not being affected. We reasoned that if centriole amplification occurred also in V(n)pp/V(n)pa as it did in V(n)p, then more than 6 centriolar foci should be present in anaphase/telophase, perhaps 9 if each parental centriole again yielded two procentrioles. In contrast to this prediction, however, we found that GFP::ZYG-1 V(n)pp/V(n)pa anaphase/telophase cells harbored no more than 6 centriolar foci (Fig. 2H, Fig. S2E). We conclude that no further centriolar amplification event occurs in the V(n)pp pa cell cycle.

We observed also that V(n)pp/pa cells in GFP::ZYG-1 animals usually assembled a tripolar spindle (Fig. 2E, I). This indicates that the extra centrosomes have MTOC activity and that they cannot cluster. As shown in Fig. 2F, such tripolar spindles generated aneuploid daughter nuclei at the end of mitosis. Therefore, in contrast to human cells and *Drosophila* (Basto et al., 2008; Ganem et al., 2009; Silkworth et al., 2009), *C. elegans* seam cells do not possess robust enough mechanisms to cluster excess centrosomes during mitosis to ensure spindle bipolarity.

Overall, we conclude that centriole amplification driven by GFP::ZYG-1 overexpression is limited to the V(n)p cell cycle preceding the sole symmetric division in the seam cell lineage, and does not occur in the asymmetric divisions occurring either before or after that (Fig. 2J).

2.3. Cell fate after tripolar spindle formation

We set out to address whether the fate of the nuclei deriving from the tripolar division of V(n)pp/pa cells was altered. In the wild-type, the anterior daughter cell differentiates and fuses with the hyp7 syncytium, whereas the posterior daughter retains the seam fate (Fig. 3A, B, ctrl). We found that this pattern was not altered amongst daughter nuclei of the tripolar division of V(n)pa/pa cells expressing GFP::ZYG-1, since the nucleus laying most anterior fused with the hyp7 syncytium, whereas the posterior-most nuclei retained the seam fate, also in cells that had undergone tripolar divisions (Fig. 3A, B, GFP::ZYG-1).

We also set out to assess whether the aneuploid daughter cells deriving from the tripolar division of V(n)pp/V(n)pa continued to proliferate. To this end, we counted the number of seam cell nuclei, either full or partial, present at the fourth larval stage. As reported in Fig. 3C-E, we rarely observed the correct number of 16 seam cell nuclei that are present in control animals (Fig. 3C, E). Instead, we usually

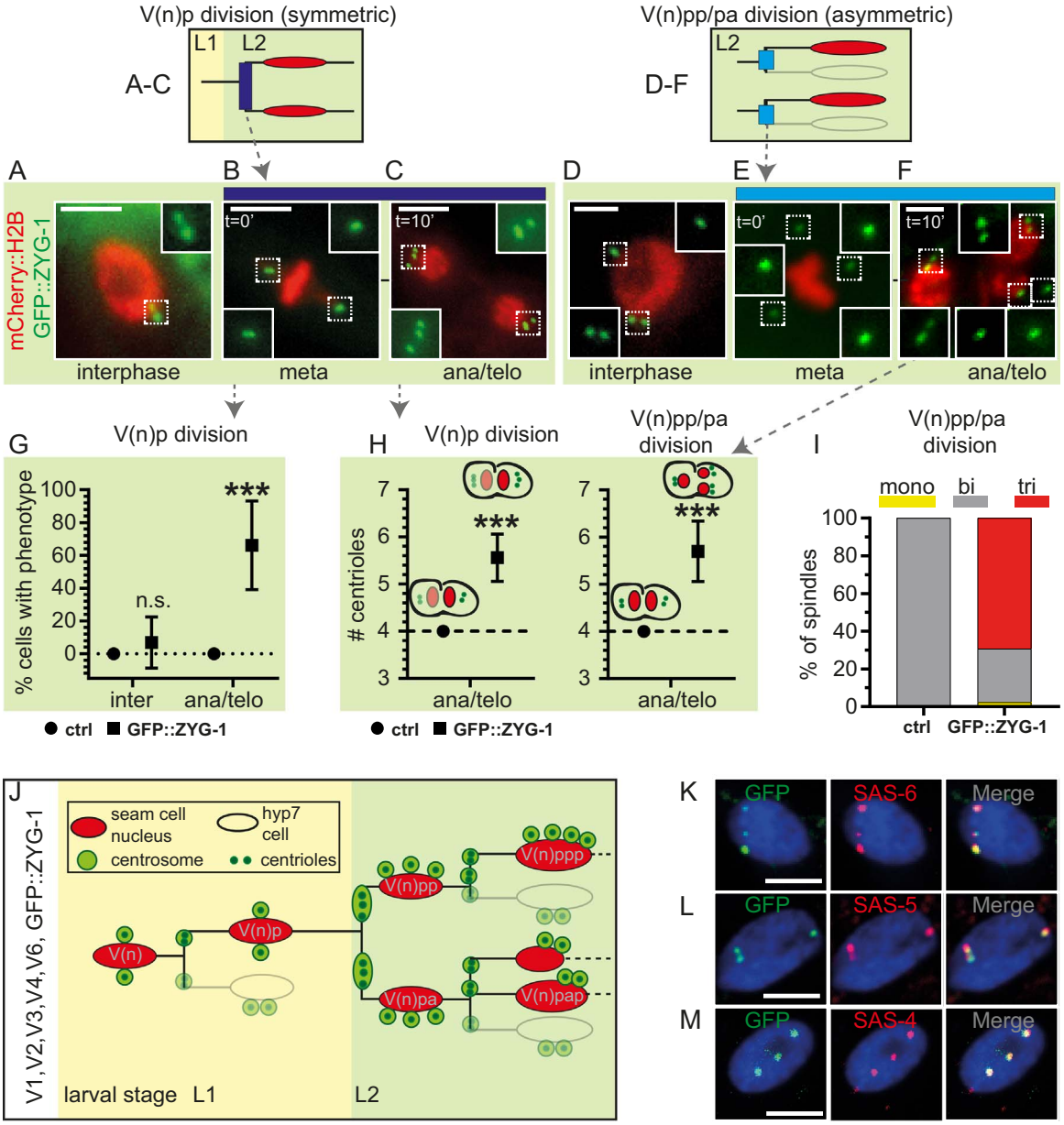

Fig. 2. ZYG-1 overexpression triggers supernumerary centrioles in V(n)p prior to symmetric division. A-F Stills images from live larvae expressing GFP::ZYG-1, shown in V(n)p **(A-C),** as well as in V(n)pp/pa **(D-F)**. Seam cell specific mCherry::H2B is seen in red, GFP::ZYG-1 in green. The interphase images are from distinct cells, the metaphase and anaphase/telophase image pairs from the same cells (with t=0 corresponding approximately to the metaphase to anaphase transition). Scale bar: 10 µm. **G** Percentage of V(n)p cells exhibiting centrosome amplification as evidenced by more than 2 GFP::ZYG-1 foci per cell in interphase or more than 4 GFP::ZYG-1 foci per cell in anaphase/telophase. N cells: ctrl 428 (interphase) and 338 (ana/telo), GFP::ZYG-1 768 (interphase) and 227 (ana/telo); Student's *t*-test with Welch correction, ***p < 0.001, n.s. not significant; interphase worms were scored 9 h after hatching. **H** Number of GFP::ZYG-1 foci per cell in anaphase/telophase, comparing V(n)p (left) and V(n)pp/pa (right) in control worms with worms expressing GFP::ZYG-1, as indicated. N worms analyzed left: ctrl, 18; GFP::ZYG-1, 307; N right: ctrl, 27; GFP::ZYG-1, 35; Student's *t*-test with Welch correction, ***p < 0.001. **I** Fraction of V(n)pp/pa mitotic cells exhibiting monopolar, bipolar or tripolar spindle configurations, as indicated. Number of worms and cells scored, respectively: control, 42, 100; GFP::ZYG-1, 45, 127; Student's *t*-test with Welch correction, ***p < 0.001. **J** Schematic representation of seam cell division pattern across larval development in GFP::ZYG-1 expressing worms, as well as centriole and centrosome numbers. See Fig. 1B for further details. **K-M** Dual immunofluorescence analysis of V4pp interphase cell expressing notably GFP::ZYG-1 with antibodies against GFP (green) and against SAS-6 **(K)**, SAS-5 **(L)** or SAS-4 **(M)**, all shown in red; DNA is shown in blue. Scale bar: 10 µm.

found less or more than that, with frequent occurrences of smaller than normal nuclei of uneven sizes (Fig. 3D, E). Moreover, we found a propensity for some seam cell nuclei to be entirely missing (Fig. 3F), a phenotype that became more prevalent in older larvae (Fig. 3G). Furthermore, less nuclei than normal differentiated into the hyp7 fate by the end of larval development in GFP::ZYG-1-expressing worms (Fig. 3D-F).

Together, the above observations indicate that the tripolar division of V(n)pp/pa cells generates aneuploid daughter nuclei that have the correct fate initially, but which do not contribute to the tissue in a normal fashion thereafter, possibly because they cease proliferating or undergo cell death.

2.4. Centriole amplification is limited to the cell cycle yielding a symmetric division

We set out to investigate why centriole amplification occurs only during the V(n)p cell cycle that precedes the symmetric division, and not during the cell cycles that yield asymmetric cell division just before or just after that. We wondered whether such differential impact is due to GFP::ZYG-1 levels being highest in V(n)p. However, quantification of GFP::ZYG-1 levels at centrosomes, where the kinase is thought to act (O'Connell et al., 2001), established that this is not the case (Fig. S3A, S3B). In addition, cytoplasmic GFP::ZYG-1 levels did not vary much,

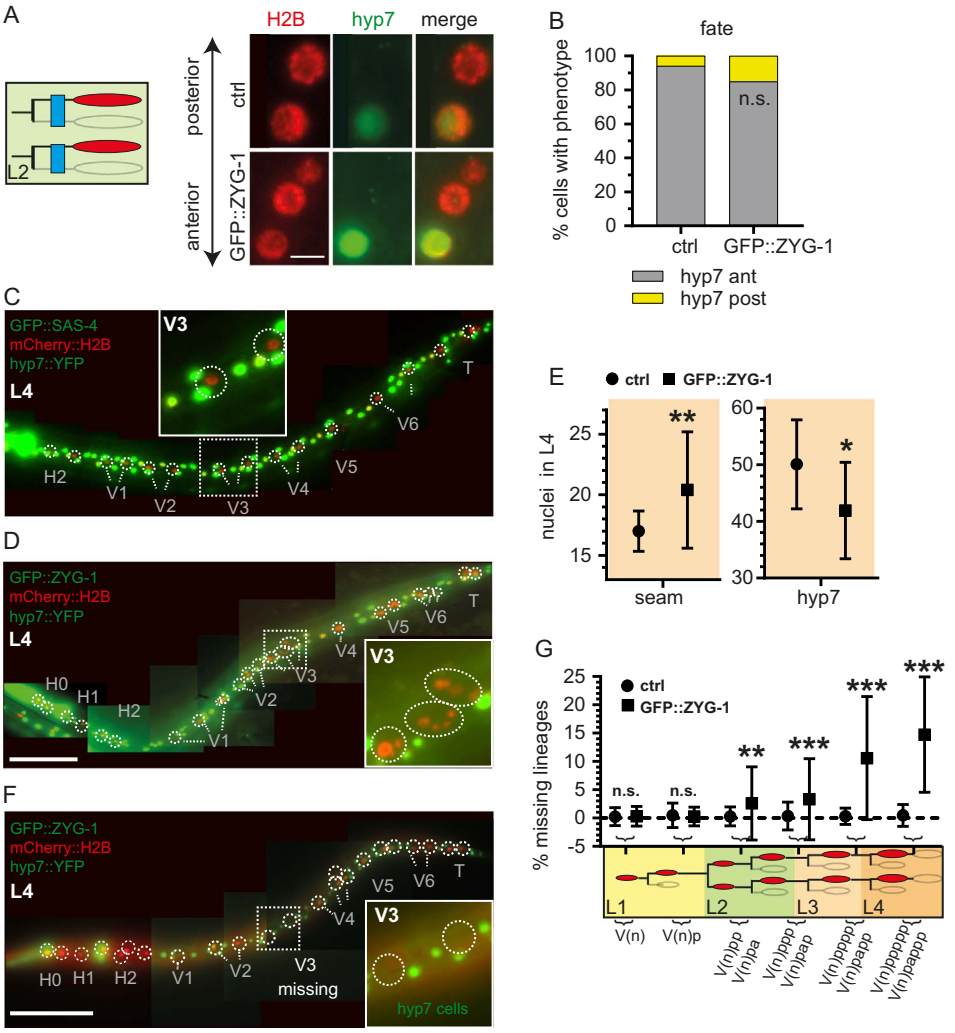

Fig. 3. Seam cell fate following centriole amplification. A Still images from live recordings of V(n)pp/pa control (top row) and GFP::ZYG-1 expressing (lower row) worms; mCherry::H2B in seam cells (red) and hyp7::YFP (green) are shown. Scale bar: 10 µm. **B** Quantification of data illustrated in (**A**), expressed as percentage of cells exhibiting either the anticipated differentiation pattern (grey), with the anterior-most nucleus (hyp7 ant) differentiating after the asymmetric division, or an abnormal differentiation pattern (yellow), with the posterior most cell (hyp7 post) differentiating. N worms; ctrl: 34, GFP::ZYG-1: 32, Student's *t*-test, n.s. non significant. **C, D, F** Still images from live recordings of L4 worms expressing in seam cells mCherry::H2B (red, chromosomes, DNA) and GFP::SAS-4 (not visible at this magnification), as well hyp7::YFP (green, hypodermis), either in a control animal **(C)** or in animals expressing GFP::ZYG-1 **(D,F).** Circles are drawn around seam cells. Scale bar: 100 µm. Inset in **(D)** shows V3 lineages with multiple micronuclei, inset in **(F)** missing V3 lineages; compare to inset in **(C)**. **E** Quantification of number of seam (left) or hypodermal (right) nuclei at the end of the L4 larval stage. Student's *t*-test with Welch correction, $^{**}p < 0.01$, $^{*}p < 0.05$. N worms: ctrl: 34; GFP::ZYG1: 20. **G** Quantification of missing seam lineages in control and GFP::ZYG-1 animals at indicated developmental stages. Numbers of worms analyzed for ctrl/GFP::ZYG-1: V(n), 40/33, V(n)p, 62/37, V(n)pp/pa, 70/73, V(n)ppp/pap, 70/57, V(n)pppp/papp, 81/17, V(n)ppppp/pappp, 64/19; multiple *t*-test of dataset with Welch correction, $^{**}p < 0.01$, $^{***}p < 0.001$, n.s. not significant; y-axis shows the percentage of missing lineages per worm.

apart from being somewhat lower in V(n)pp/pa (Fig. S3C, S3D). Taken together, these experiments concur to show that supernumerary centrioles do not form strictly in V(n)p because of differences in GFP::ZYG-1 protein levels.

In seeking an alternative explanation, we wondered whether such uniqueness might reflect the special fate of V(n)p, since this is the only cell in the seam lineage yielding a symmetric division (Fig. 4A). To test this hypothesis, we first examined animals depleted by RNAi of the heterochronic gene *lin-14*. In this case, the seam lineage skips the V(n) asymmetric division that normally occurs during the L1 stage, and instead begins larval development directly with a cell expressing a fate akin to that of V(n)p, yielding a symmetric division already 2 h after hatching (Fig. 4D, Sulston and Horvitz, 1981). Strikingly, we found that centriole amplification driven by GFP::ZYG-1 begins already in this first cell upon LIN-14 depletion (Fig. 4A-C for *ctrl(RNAi)*, Fig. 4D-F for *lin-14(RNAi)* and Fig. 4G, H for quantification). We conclude that a precocious V(n)p-like seam cell fate leading to symmetric division is sufficient to promote supernumerary centriole formation.

We next set out to test whether a V(n)p-like fate might also be necessary for centriole amplification upon GFP::ZYG-1 expression. To do so, we analyzed animals depleted of LIN-28, in which L2 fates are skipped, such that animals proceed directly from the L1 to the L3 larval stages, without undergoing symmetric divisions in the seam lineage (Fig. 4I, Ambros, 1989; Balzer et al., 2010; Sulston and Horvitz, 1981). Strikingly, we found that GFP::ZYG-1 expression did not provoke substantial centriole amplification in *lin-28(RNAi)* animals (Fig. 4J-M).

Overall, these experiments indicate that the fate of V(n)p, the sole cell in the V seam cell lineage that yields a symmetric cell division, is both sufficient and necessary to enable extra centrioles to be formed upon excess GFP::ZYG-1, leading to aneuploidy and defective development.

3. Discussion

Using *C. elegans* seam cells as a model system to probe the consequence of centriole amplification in an invertebrate stem cell

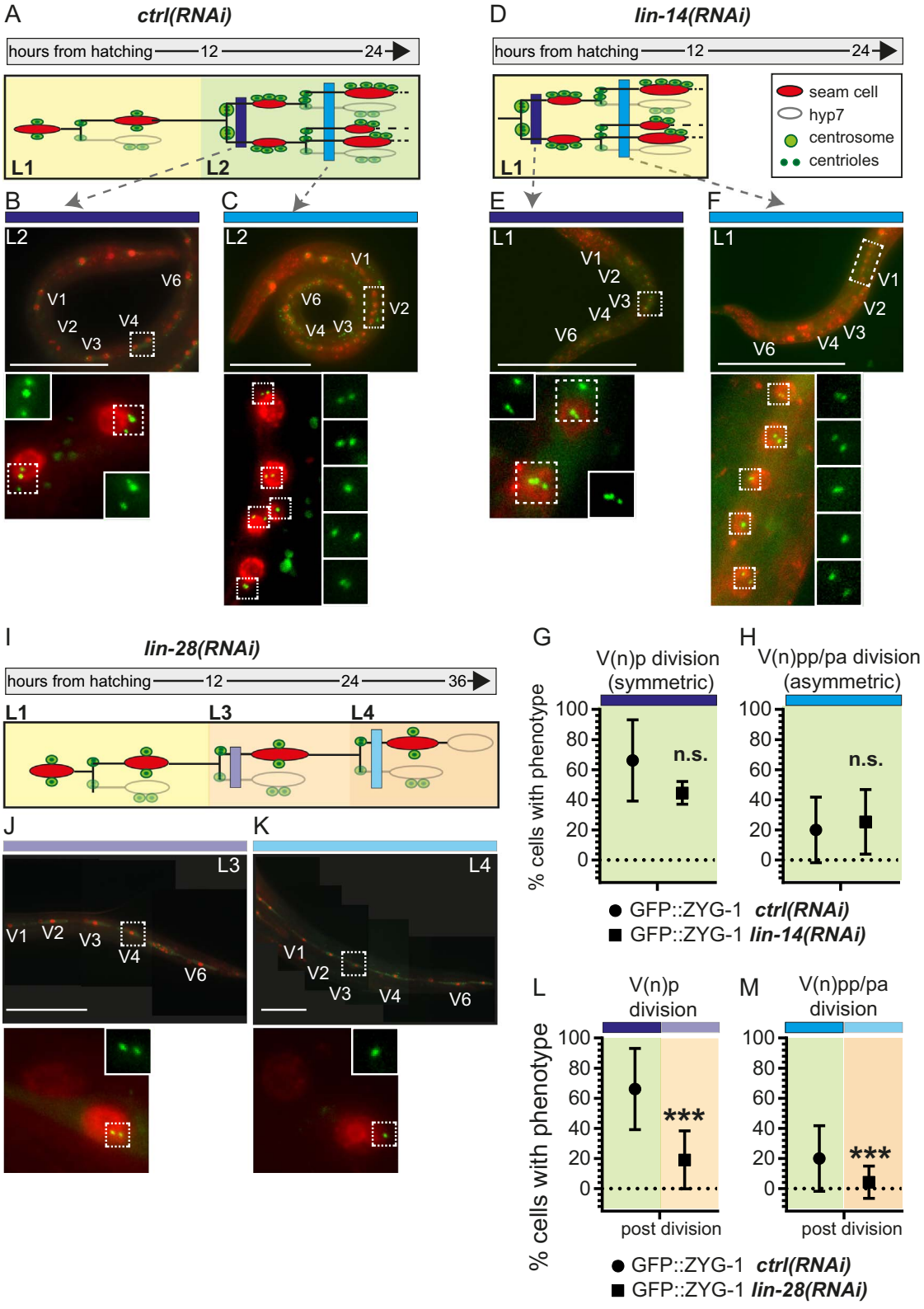
A
ctrl(RNAi)
hours from hatching
12
24
L1
L2
B
C
V1
V2
V3
V4
V6
D
lin-14(RNAi)
seam cell
hyp7
centrosome
centrioles
E
F
I
lin-28(RNAi)
36
L3
L4
J
K
G
V(n)p division (symmetric)
H
V(n)pp/pa division (asymmetric)
% cells with phenotype
n.s.
GFP::ZYG-1 ctrl(RNAi)
GFP::ZYG-1 lin-14(RNAi)
L
V(n)p division
M
V(n)pp/pa division
***
post division
GFP::ZYG-1 ctrl(RNAi)
GFP::ZYG-1 lin-28(RNAi)

Fig. 4. Centriole amplification is limited to the seam cell cycle yielding a symmetric division A, D, I Schematics of larval development in animals expressing GFP::ZYG-1 in seam cells and subjected to control RNAi **(A)**, *lin-14(RNAi)* **(D),** where larval development starts with the symmetric seam cell division and the L1 division events are skipped, as well as *lin-28*(*RNAi*) **(I)**, where the divisions of the second larval stage are skipped and worms undergo only asymmetric seam cell divisions. Seam cell nuclei are depicted in red, hyp7 nuclei as empty circles; centrosomes and centrioles are shown in green. The dark blue bar **(A, B)** represents a time point after the symmetric seam cell division, the light blue bar after the following asymmetric division **(A, B)**. In **I**, the lilac bar indicates a time point after the asymmetric seam cell division that happens instead of a symmetric division in *lin-28* depleted animals, the very light blue bar the time point after the following asymmetric division **(I). B, C** L2 *ctrl(RNAi)* worm expressing GFP::ZYG-1 and mCherry::H2B in seam cells after the symmetric seam cell division (**B**, dark blue bar in **A**) and following asymmetric seam cell division (**C**, light blue bar in **A**). Magnified insets show the V4 **(B)** and V2 **(C)** lineages, respectively. Scale bar: 100 μm. **E, F** L1 *lin-14(RNAi)* worm expressing GFP::ZYG-1 and mCherry::H2B in seam cells after the symmetric seam cell division (**E**, dark blue bar in **D**) and following asymmetric seam cell division (**F**, light blue bar in **D**). Magnified insets show the V3 **(E)** and V1 (**F**) lineages, respectively. Scale bar: 100 μm. **G** Quantification of cells with phenotype after the symmetric seam cell division (corresponding to the dark blue bar); Student's *t*-test with Welch correction. N.s. not significant. N lineages: ctrl (see Fig. 2G ana/telo), 227; *lin-14(RNAi)*, 36. **H** Quantification of cells with phenotype after the asymmetric seam cell division (corresponding to the light blue bar in A and D); Student's *t*-test with Welch correction, n.s. not significant; n lineages: ctrl, 174; *lin-14(RNAi)*, 143. **J**, **K** L3 **(J)** and L4 **(K)** *lin-28(RNAi)* worms expressing GFP::ZYG-1 and mCherry::H2B in seam cells after the V(n)p seam cell division, which is symmetric in ctrl animals and asymmetric in *lin-28(RNAi)* (**J**, lilac bar in **I**) and following asymmetric seam cell division (**K**, light blue bar in **I**). Magnified insets show the V4 **(J)** and V3 **(K)** lineages. Scale bar: 100 μm. **L** Quantification of cells with phenotype after the first division following the L1 divisions (V(n)p), which is a symmetric division in ctrl (**B**, dark blue) and an asymmetric division upon LIN-28 depletion (**J**, lilac bar); Student's *t*-test with Welch correction, ***p < 0.001; N lineages: ctrl, 227; *lin-28*(*RNAi*), 105. **M** Quantification of cells with phenotype after the second division following the L1 divisions (V(n)pp/pa), which is an asymmetric division in ctrl condition (**C**, light blue) and an asymmetric division upon LIN-28 depletion (**K**, light blue); Student's *t*-test with Welch correction, ***p < 0.001; N lineages: ctrl, 174; *lin-28*(*RNAi*), 83.

lineage, we found that one supernumerary procentriole forms per parental centriole upon GFP::ZYG-1 expression in cells that divide symmetrically. These findings provide the first evidence, to our knowledge, that supernumerary centrioles can be generated in worm somatic cells, and provide a novel system for investigating the mechanisms through which an organism handles centrosome number aberrations in stem cells.

Although supernumerary centrioles have not been observed previously in somatic cells of *C. elegans*, it has been reported that down-regulation of Protein Phosphatase I function in early embryos results in the presence of excess centrioles, owing to increased ZYG-1 levels (Peel et al., 2017). In the embryo, this effect is not restricted to a single cell cycle, in contrast to the situation in seam cells reported here. Why could the effect be restricted to the V(n)p cells that undergo symmetric division and not affect cells that precede or follow, both of which undergo asymmetric division? We found that this cannot be attributed to differences in GFP::ZYG-1 levels. This is in line with the fact that the seam cell promoter is active already when the first seam cells are born during embryogenesis (Gorrepati et al., 2013; Sulston et al., 1983). The fact that supernumerary centrioles are formed earlier in *lin-14*(*RNAi*) larvae further indicates that sufficient GFP::ZYG-1 is present at an earlier time to potentially have an impact. Therefore, the data taken together suggests instead that some feature of the V(n)p symmetric cell cycle makes it more sensitive than the bounding asymmetric cell cycles to the presence of excess ZYG-1. While identifying the nature of this feature will require further investigations, one possibility is that a ZYG-1 partner or substrate is missing or present in an insufficient manner in the asymmetric cell cycles. For instance, in human cells and in *Drosophila*, the ZYG-1-related kinase Plk4 functions during centriole formation by phosphorylating the SAS-5-related proteins STIL and Ana2, respectively (Dzhindzhev et al., 2014; Ohta et al., 2014). Perhaps SAS-5 is present at a lesser level or does not operate sufficiently well to allow excess ZYG-1 to be effective during the asymmetric cell cycles of the seam lineage.

Regardless of the mechanism that restricts the impact of excess ZYG-1 to the symmetrically dividing cell, it is interesting to note that just one extra procentriole forms in the vicinity of each parental centriole. This is in contrast to the situation in S-phase-arrested human cells, where overexpression of Plk4 can result in the formation, around the parental centriole, of characteristic rosettes that contain up to 6 procentrioles (Comartin et al., 2013; Habedanck et al., 2005). How can the difference with the situation in *C. elegans* seam cells be explained? Although other hypotheses can be envisaged, a simple possible explanation derives from mere geometric considerations. Procentrioles in human cells emanate from a large torus that contains notably Cep152, and which has been estimated to be ~435 nm in outer diameter (Lawo et al., 2012). Considering that human centrioles are ~250 nm in outer diameter, it follows that there is enough space in principle for 5–6 procentrioles to emerge from a Cep152-containing torus. By contrast, a structure neatly surrounding the much smaller *C. elegans* centriole, which is ~150 nm in outer diameter (Pelletier et al., 2006), might not offer sufficient space for more than one extra procentriole to emerge, even with excess ZYG-1.

Cells confronted with too many centrosomes often cluster them during mitosis, which ensures spindle bipolarity and promotes relatively equal segregation of the genetic material to daughter cells (Ganem et al., 2009; Quintyne et al., 2005; Silkworth et al., 2009). Efficient clustering relies notably on an intact actin cytoskeleton, on the spindle assembly checkpoint, and on the activity of the HSET family of kinesins (Basto et al., 2008; Ganem et al., 2009; Kwon et al., 2008; Silkworth et al., 2009). We uncovered here that clustering mechanisms are not robust enough in the seam lineage to buffer the consequences of extra centrosomes, and it will be interesting to investigate whether this is due to modulation of the actin cytoskeleton, of the spindle assembly checkpoint, of HSET kinesins or yet for another reason. Regardless, the consequences of not being able to achieve such clustering are dire because aneuploidy ensues. This outcome is reminiscent of the situation in the developing mouse neocortex (Marthiens et al., 2013). While effective at suppressing faulty cells from a population, such lack of clustering leads to severe defects in organogenesis in seam and hypodermal cells in *C. elegans*, as it does in mammalian neural stem cells. Intriguingly, some microcephaly-causing mutations in STIL result in an overactive protein (Arquint and Nigg, 2014), raising the possibility that faulty clustering also contributes to this dramatic human disease condition.

In conclusion, our work uncovered that extra centrosomes form strictly in some cells of a stereotyped stem cell lineage in *C. elegans*, raising the possibility that similar restricted consequences may operate in other systems and help explain the interplay between centrosome number aberrations and proliferation control.

4. Materials and methods

4.1. Nematode strains

C. elegans culture was according to standard procedures (Brenner, 1974). All transgenic animals were generated by integrating the constructs described below in the genome as per standard methods (Praitis et al., 2001).

In order to generate the control strain expressing GFP::SAS-4 and mCherry::H2B in seam cells, as well as YFP::hyp-7 in hypodermal cells, *mCherry::h2b* was PCR-amplified from pCM1.151 (gift from Geraldine Seydoux, Merritt et al., 2008), *gpf::sas-4* from pSU25-*gfp::sas-4* (Leidel and Gönczy, 2003), and each cloned into a multi-Gateway plasmid pDONR221 (Thermo Fisher Scientific). The pSCM promoter and the *unc-54* 3' UTR were PCR-amplified from pSCM:lacZ:unc54UTR (gift from

Alison Woollard) and cloned into the Gateway plasmids pDONR P4-P1R and pDONR P2R-P3, respectively. Combinations of either pDONR221 plasmid, as well as the pDONR P4-P1R-pSCM and pDONR P2R-P3-unc-54UTR plasmids, were used to assemble the final constructs into the multi-Gateway plasmid pCG150. After co-bombardement of worms with pCG150 containing either *gfp::sas-4*, with pSCM and *unc-54* 3' UTR, or *mCherry::h2b*, with pSCM and *unc-54* 3'UTR, the resulting worm strain GZ1162 containing mCherry::H2B and GFP::SAS-4 (of genotype isIS41[SCMp::mCHerry:H2B *unc-119*(+)], isIS42[SCMp::GFP::SAS-4 *unc-119*(+)]), was crossed with strains GS3798 (of genotype *arls99*[*dpy-7p*::2Xnls::yfp], (Myers and Greenwald, 2005) and CB3855 (of genotype *plg-1*(*e2001*) III; *him-5*(*e1490*) V (Barrett et al., 2004) to obtain homozygous animals of the genotype isIS41[SCMp::mCHerry::H2B *unc-119*(+)], isIS42[SCMp::GFP::SAS-4 *unc-119*(+)]; *plg-1*(*e2001*) III, *him-5*(*e1490*) V, *arls99*[*dpy-7p*::2X*nls::yfp*) (strain GZ1230).

To generate strains overexpressing GFP::ZYG-1 in seam cells, *gfp*::*zyg-1* was PCR-amplified from pSU25-*gfp*::*zyg-1* (Leidel, 2005) and also cloned into pDONR221; pDONR P4-P1R-pSCM and pDONR P2R-P3-unc-54 3'UTR were used to assemble a final construct into the multi-Gateway plasmid pCG150 containing GFP::ZYG-1 and bombarded as described above. The resulting strain GZ1183 of genotype [isIS43[SCMp::GFP::ZYG-1 *unc-119*(+)]] was used to assess GFP::ZYG-1 levels (see Fig. S2). For all other experiments, this strain was crossed into the control strain, removing GFP::SAS-4 in doing so, as verified by PCR (used for Figs. 2 and 3) or into OC534 (*unc-119*(*ed3*) III; *bsIs20*[pNP99: *unc-119*(+) *tbb-1p-mCherry-tbb-2-tbb-2* UTR]; *unc-119*(*ed3*); *bsIs2*[pCK5.5:*pie-1-gfp-spd-2*], which was a gift from Kevin O'Connell (used for Figs. 2 and 4).

To assess the impact of centriole duplication failure in seam cells, *sas-5*(*t2079*)/ *nT1*(*qIs51*) IV (Delattre et al., 2004) was crossed into the control strain. Moreover, *sas-6(ok2554)* (Kitagawa et al., 2011) was crossed into JR667 (*unc-119*(*e2498::Tc1*) III; *wIs51*[SCMp::GFP unc-119(+)] V), which expresses GFP under the seam cell promoter in the cytoplasm of seam cells.

4.2. RNAi

RNAi experiments were performed at 25 °C by feeding worms with HT115 bacteria expressing double-stranded RNA corresponding to given target genes using standard protocols (Rual et al., 2004). HT115 bacteria transformed with an empty L4440 vector were used as negative control. L4 animals were plated on RNAi plates and the next generation analyzed starting from the L1 stage, except for *sas-6*(*RNAi*), where young gravid hermaphrodites were treated and the next generation of larvae analyzed.

4.3. Live imaging

Dual time lapse differential interference contrast (DIC) and fluorescence imaging was performed on larvae placed onto 3.5 cm diameter dishes as described (Chai et al., 2012) using a Zeiss Axio Observer microscope equipped with a CoolSnap-ES2 CCD camera (6.45×6.45 pixel, 12 bit, 20 MHz, 10 frames/s) and controlled by Micro-Manager Software (Edelstein et al., 2010, 2014) or Visiview software (Visitron). Images were acquired at 30–100 ms exposure times using 7% laser power.

For long-term monitoring of larvae, worms were transferred back to feeding plates between imaging time points to allow molting, and transferred again at the appropriate time points for subsequent imaging. Lineage analysis was performed as previously described (Sulston and Horvitz, 1977). Seam cell nuclei were identified by the presence of mCherry::H2B expressed under the pSCM seam cell promoter.

4.4. Immunofluorescence

Synchronized larvae were washed and re-suspended in dH2O; ~5 µl of this suspension was then deposited onto slides coated with 2 µg/µl poly-L-lysine in PBS. An 18 mm^2 coverslip was placed onto the drop and excess fluid was wicked away with 3MM Whatman paper. Thereafter, the slide was frozen on a block of metal precooled on packed dry ice. After a few minutes, the coverslip was flicked off with a razor blade, and the slide plunged into −20 °C methanol for 5 min before rehydrating in an Acetone/Ethanol series. The samples were blocked for 1 h with 1% BSA 0.05% Tween-20 in PBS, incubated with primary antibodies overnight at 4 °C, washed and then incubated with secondary antibodies for 1 h at room temperature.

The following primary antibodies raised in rabbit were used: 1:800 SAS-4 (Leidel and Gönczy, 2003), 1:50 SAS-5 (Delattre et al., 2004), 1:1000 SAS-6 (Leidel et al., 2005), 1:1000 ZYG-1 (Leidel and Gönczy, 2003), as well as 1:500 mouse anti-GFP (Molecular Probes). Secondary antibodies were 1:1000 goat anti-rabbit coupled to Alexa 568 and 1:500 goat anti-mouse coupled to Alexa 488. Slides were counterstained with ~1 µg/ml Hoechst 33258 (Sigma) to visualize DNA. Indirect immunofluorescence was imaged on an LSM700 Zeiss confocal microscope, using relevant 0.5–1 µm optical slices. Images were processed using ImageJ (Schindelin et al., 2012; Schneider et al., 2012).

4.5. Statistical analysis

Statistical analysis was performed using GraphPad Prism (Version 7.01). Unpaired two-tailed Student's *t*-tests with Welch correction were used to determine significance between two groups of data in the same set of experiments.

Acknowledgements

We are grateful to Serena Ding, Martin Eilers, Samantha Hughes, Michel Labouesse and Alisson Woollard for useful discussions, to Coralie Busso for generating transgenic animals, as well as to Alexandra Bezler and Marie Pierron for comments on the manuscript. For worm strains and plasmids, we thank Kevin O'Connell, Geraldine Seydoux and Alisson Woollard, as well as the *Caenorhabditis* Genetics Center, which is funded by the NIH National Center for Research Resources (NCRR, P40 OD010440).

Funding

This work was funded by a Mildred-Scheel (110470, German Cancer Aid) postdoctoral fellowship to B.W.Author contributions

B.W., P.G. and F.B. designed the study. B.W. performed the experiments. F.B. cloned fusion vectors used for bombardments. B.W. and A.S. analyzed the data. B.W. and P.G. wrote the manuscript.

Appendix A. Supporting information

Supplementary data associated with this article can be found in the online version at doi:10.1016/j.ydbio.2018.01.001.

References

Ambros, V., 1989. A hierarchy of regulatory genes controls a larva-to-adult developmental switch in C. elegans. Cell 57, 49–57.
Ambros, V., 2000. Control of developmental timing in Caenorhabditis elegans. Curr. Opin. Genet. Dev. 10, 428–433.
Ambros, V., Horvitz, H.R., 1984. Heterochronic mutants of the nematode Caenorhabditis elegans. Science 226, 409–416.
Ambros, V., Horvitz, H.R., 1987. The lin-14 locus of Caenorhabditis elegans controls the time of expression of specific postembryonic developmental events. Genes Dev. 1, 398–414.
Arquint, C., Nigg, E.A., 2014. STIL microcephaly mutations interfere with APC/C-

mediated degradation and cause centriole amplification. Curr. Biol.: CB 24, 351–360.
Arquint, C., Sonnen, K.F., Stierhof, Y.D., Nigg, E.A., 2012. Cell-cycle-regulated expression of STIL controls centriole number in human cells. J. Cell Sci. 125, 1342–1352.
Balzer, E., Heine, C., Jiang, Q., Lee, V.M., Moss, E.G., 2010. LIN28 alters cell fate succession and acts independently of the let-7 microRNA during neurogliogenesis in vitro. Development 137, 891–900.
Barrett, P.L., Fleming, J.T., Gobel, V., 2004. Targeted gene alteration in Caenorhabditis elegans by gene conversion. Nat. Genet. 36, 1231–1237.
Basto, R., Brunk, K., Vinadogrova, T., Peel, N., Franz, A., Khodjakov, A., Raff, J.W., 2008. Centrosome amplification can initiate tumorigenesis in flies. Cell 133, 1032–1042.
Bornens, M., 2012. The centrosome in cells and organisms. Science 335, 422–426.
Brenner, S., 1974. The genetics of Caenorhabditis elegans. Genetics 77, 71–94.
Brito, D.A., Gouveia, S.M., Bettencourt-Dias, M., 2012. Deconstructing the centriole: structure and number control. Curr. Opin. Cell Biol. 24, 4–13.
Chai, Y., Li, W., Feng, G., Yang, Y., Wang, X., Ou, G., 2012. Live imaging of cellular dynamics during Caenorhabditis elegans postembryonic development. Nat. Protoc. 7, 2090–2102.
Chalfie, M., Horvitz, H.R., Sulston, J.E., 1981. Mutations that lead to reiterations in the cell lineages of C. elegans. Cell 24, 59–69.
Coelho, P.A., Bury, L., Shahbazi, M.N., Liakath-Ali, K., Tate, P.H., Wormald, S., Hindley, C.J., Huch, M., Archer, J., Skarnes, W.C., Zernicka-Goetz, M., Glover, D.M., 2015. Over-expression of Plk4 induces centrosome amplification, loss of primary cilia and associated tissue hyperplasia in the mouse. Open Biol. 5, 150209.
Comartin, D., Gupta, G.D., Fussner, E., Coyaud, E., Hasegan, M., Archinti, M., Cheung, S.W., Pinchev, D., Lawo, S., Raught, B., Bazett-Jones, D.P., Luders, J., Pelletier, L., 2013. CEP120 and SPICE1 cooperate with CPAP in centriole elongation. Curr. Biol.: CB 23, 1360–1366.
Dammermann, A., Muller-Reichert, T., Pelletier, L., Habermann, B., Desai, A., Oegema, K., 2004. Centriole assembly requires both centriolar and pericentriolar material proteins. Dev. Cell 7, 815–829.
Delattre, M., Leidel, S., Wani, K., Baumer, K., Bamat, J., Schnabel, H., Feichtinger, R., Schnabel, R., Gönczy, P., 2004. Centriolar SAS-5 is required for centrosome duplication in C. elegans. Nat. Cell Biol. 6, 656–664.
Dzhindzhev, N.S., Tzolovsky, G., Lipinszki, Z., Schneider, S., Lattao, R., Fu, J., Debski, J., Dadlez, M., Glover, D.M., 2014. Plk4 phosphorylates Ana2 to trigger Sas6 recruitment and procentriole formation. Curr. Biol.: CB 24, 2526–2532.
Edelstein, A., Amodaj, N., Hoover, K., Vale, R., Stuurman, N., 2010. Computer control of microscopes using micromanager. Curr. Protoc. Mol. Biol. 20, (Chapter 14, Unit14).
Edelstein, A.D., Tsuchida, M.A., Amodaj, N., Pinkard, H., Vale, R.D., Stuurman, N., 2014. Advanced methods of microscope control using muManager software. J. Biol. Methods 1.
Firat-Karalar, E.N., Stearns, T., 2014. The centriole duplication cycle. Philos. Trans. R. Soc. Lond. Ser. B Biol. Sci. 369.
Ganem, N.J., Godinho, S.A., Pellman, D., 2009. A mechanism linking extra centrosomes to chromosomal instability. Nature 460, 278–282.
Gleason, J.E., Eisenmann, D.M., 2010. Wnt signaling controls the stem cell-like asymmetric division of the epithelial seam cells during C. elegans larval development. Dev. Biol. 348, 58–66.
Gönczy, P., 2012. Towards a molecular architecture of centriole assembly. Nat. Rev. Mol. Cell Biol. 13, 425–435.
Gorrepati, L., Thompson, K.W., Eisenmann, D.M., 2013. C. elegans GATA factors EGL-18 and ELT-6 function downstream of Wnt signaling to maintain the progenitor fate during larval asymmetric divisions of the seam cells. Development 140, 2093–2102.
Ha, I., Wightman, B., Ruvkun, G., 1996. A bulged lin-4/lin-14 RNA duplex is sufficient for Caenorhabditis elegans lin-14 temporal gradient formation. Genes Dev. 10, 3041–3050.
Habedanck, R., Stierhof, Y.D., Wilkinson, C.J., Nigg, E.A., 2005. The Polo kinase Plk4 functions in centriole duplication. Nat. Cell Biol. 7, 1140–1146.
Joshi, P.M., Riddle, M.R., Djabrayan, N.J., Rothman, J.H., 2010. Caenorhabditis elegans as a model for stem cell biology. Dev. Dyn.: Off. Publ. Am. Assoc. Anat. 239, 1539–1554.
Kagoshima, H., Nimmo, R., Saad, N., Tanaka, J., Miwa, Y., Mitani, S., Kohara, Y., Woollard, A., 2007. The C. elegans CBFbeta homologue BRO-1 interacts with the Runx factor, RNT-1, to promote stem cell proliferation and self-renewal. Development 134, 3905–3915.
Kagoshima, H., Sawa, H., Mitani, S., Burglin, T.R., Shigesada, K., Kohara, Y., 2005. The C. elegans RUNX transcription factor RNT-1/MAB-2 is required for asymmetrical cell division of the T blast cell. Dev. Biol. 287, 262–273.
Kemp, C.A., Kopish, K.R., Zipperlen, P., Ahringer, J., O'Connell, K.F., 2004. Centrosome maturation and duplication in C. elegans require the coiled-coil protein SPD-2. Dev. Cell 6, 511–523.
Kirkham, M., Muller-Reichert, T., Oegema, K., Grill, S., Hyman, A.A., 2003. SAS-4 is a C. elegans centriolar protein that controls centrosome size. Cell 112, 575–587.
Kitagawa, D., Fluckiger, I., Polanowska, J., Keller, D., Reboul, J., Gonczy, P., 2011. PP2A phosphatase acts upon SAS-5 to ensure centriole formation in C. elegans embryos. Dev. Cell 20, 550–562.
Kwon, M., Godinho, S.A., Chandhok, N.S., Ganem, N.J., Azioune, A., Thery, M., Pellman, D., 2008. Mechanisms to suppress multipolar divisions in cancer cells with extra centrosomes. Genes Dev. 22, 2189–2203.
Lawo, S., Hasegan, M., Gupta, G.D., Pelletier, L., 2012. Subdiffraction imaging of centrosomes reveals higher-order organizational features of pericentriolar material. Nat. Cell Biol. 14, 1148–1158.
Leidel, S., Delattre, M., Cerutti, L., Baumer, K., Gönczy, P., 2005. SAS-6 defines a protein family required for centrosome duplication in C. elegans and in human cells. Nat. Cell Biol. 7, 115–125.
Leidel, S., Gönczy, P., 2003. SAS-4 is essential for centrosome duplication in C elegans and is recruited to daughter centrioles once per cell cycle. Dev. Cell 4, 431–439.
Levine, M.S., Bakker, B., Boeckx, B., Moyett, J., Lu, J., Vitre, B., Spierings, D.C., Lansdorp, P.M., Cleveland, D.W., Lambrechts, D., Foijer, F., Holland, A.J., 2017. Centrosome Amplification Is Sufficient to Promote Spontaneous Tumorigenesis in Mammals. Dev. Cell 40, 313–322, (e315).
Marthiens, V., Rujano, M.A., Pennetier, C., Tessier, S., Paul-Gilloteaux, P., Basto, R., 2013. Centrosome amplification causes microcephaly. Nat. Cell Biol. 15, 731–740.
Merritt, C., Rasoloson, D., Ko, D., Seydoux, G., 2008. 3' UTRs are the primary regulators of gene expression in the C. elegans germline. Curr. Biol.: CB 18, 1476–1482.
Mizumoto, K., Sawa, H., 2007. Two betas or not two betas: regulation of asymmetric division by beta-catenin. Trends Cell Biol. 17, 465–473.
Moss, E.G., Lee, R.C., Ambros, V., 1997. The cold shock domain protein LIN-28 controls developmental timing in C. elegans and is regulated by the lin-4 RNA. Cell 88, 637–646.
Myers, T.R., Greenwald, I., 2005. lin-35 Rb acts in the major hypodermis to oppose ras-mediated vulval induction in C. elegans. Dev. Cell 8, 117–123.
Nimmo, R., Antebi, A., Woollard, A., 2005. mab-2 encodes RNT-1, a C. elegans Runx homologue essential for controlling cell proliferation in a stem cell-like developmental lineage. Development 132, 5043–5054.
Nimmo, R., Woollard, A., 2008. Worming out the biology of Runx. Dev. Biol. 313, 492–500.
O'Connell, K.F., Caron, C., Kopish, K.R., Hurd, D.D., Kemphues, K.J., Li, Y., White, J.G., 2001. The C. elegans zyg-1 gene encodes a regulator of centrosome duplication with distinct maternal and paternal roles in the embryo. Cell 105, 547–558.
Ohta, M., Ashikawa, T., Nozaki, Y., Kozuka-Hata, H., Goto, H., Inagaki, M., Oyama, M., Kitagawa, D., 2014. Direct interaction of Plk4 with STIL ensures formation of a single procentriole per parental centriole. Nat. Commun. 5, 5267.
Pasquinelli, A.E., Ruvkun, G., 2002. Control of developmental timing by micrornas and their targets. Annu. Rev. Cell Dev. Biol. 18, 495–513.
Peel, N., Iyer, J., Naik, A., Dougherty, M.P., Decker, M., O'Connell, K.F., 2017. Protein phosphatase 1 down regulates ZYG-1 levels to limit centriole duplication. PLoS Genet. 13, e1006543.
Pelletier, L., O'Toole, E., Schwager, A., Hyman, A.A., Muller-Reichert, T., 2006. Centriole assembly in Caenorhabditis elegans. Nature 444, 619–623.
Praitis, V., Casey, E., Collar, D., Austin, J., 2001. Creation of low-copy integrated transgenic lines in Caenorhabditis elegans. Genetics 157, 1217–1226.
Quintyne, N.J., Reing, J.E., Hoffelder, D.R., Gollin, S.M., Saunders, W.S., 2005. Spindle multipolarity is prevented by centrosomal clustering. Science 307, 127–129.
Rual, J.F., Hirozane-Kishikawa, T., Hao, T., Bertin, N., Li, S., Dricot, A., Li, N., Rosenberg, J., Lamesch, P., Vidalain, P.O., Clingingsmith, T.R., Hartley, J.L., Esposito, D., Cheo, D., Moore, T., Simmons, B., Sequerra, R., Bosak, S., Doucette-Stamm, L., Le Peuch, C., Vandenhaute, J., Cusick, M.E., Albala, J.S., Hill, D.E., Vidal, M., 2004. Human ORFeome version 1.1: a platform for reverse proteomics. Genome Res. 14, 2128–2135.
Schindelin, J., Arganda-Carreras, I., Frise, E., Kaynig, V., Longair, M., Pietzsch, T., Preibisch, S., Rueden, C., Saalfeld, S., Schmid, B., Tinevez, J.Y., White, D.J., Hartenstein, V., Eliceiri, K., Tomancak, P., Cardona, A., 2012. Fiji: an open-source platform for biological-image analysis. Nat. Methods 9, 676–682.
Schneider, C.A., Rasband, W.S., Eliceiri, K.W., 2012. NIH Image to ImageJ: 25 years of image analysis. Nat. Methods 9, 671–675.
Sercin, O., Larsimont, J.C., Karambelas, A.E., Marthiens, V., Moers, V., Boeckx, B., Le Mercier, M., Lambrechts, D., Basto, R., Blanpain, C., 2016. Transient PLK4 overexpression accelerates tumorigenesis in p53-deficient epidermis. Nat. Cell Biol. 18, 100–110.
Silkworth, W.T., Nardi, I.K., Scholl, L.M., Cimini, D., 2009. Multipolar spindle pole coalescence is a major source of kinetochore mis-attachment and chromosome mis-segregation in cancer cells. PloS One 4, e6564.
Strnad, P., Leidel, S., Vinogradova, T., Euteneuer, U., Khodjakov, A., Gönczy, P., 2007. Regulated HsSAS-6 levels ensure formation of a single procentriole per centriole during the centrosome duplication cycle. Dev. Cell 13, 203–213.
Sugioka, K., Hamill, D.R., Lowry, J.B., McNeely, M.E., Enrick, M., Richter, A.C., Kiebler, L.E., Priess, J.R., Bowerman, B., 2017. Centriolar SAS-7 acts upstream of SPD-2 to regulate centriole assembly and pericentriolar material formation. eLife 6.
Sulston, J.E., Horvitz, H.R., 1977. Post-embryonic cell lineages of the nematode, Caenorhabditis elegans. Dev. Biol. 56, 110–156.
Sulston, J.E., Horvitz, H.R., 1981. Abnormal cell lineages in mutants of the nematode Caenorhabditis elegans. Dev. Biol. 82, 41–55.
Sulston, J.E., Schierenberg, E., White, J.G., Thomson, J.N., 1983. The embryonic cell lineage of the nematode Caenorhabditis elegans. Dev. Biol. 100, 64–119.
Vadla, B., Kemper, K., Alaimo, J., Heine, C., Moss, E.G., 2012. lin-28 controls the succession of cell fate choices via two distinct activities. PLoS Genet. 8, e1002588.
Wolf, N., Hirsh, D., McIntosh, J.R., 1978. Spermatogenesis in males of the free-living nematode, Caenorhabditis elegans. J. Ultrastruct. Res. 63, 155–169.
Woodruff, J.B., Wueseke, O., Hyman, A.A., 2014. Pericentriolar material structure and dynamics. Philos. Trans. R. Soc. Lond. Ser. B, Biol. Sci. 369.